Available online at www.sciencedirect.com
ScienceDirect
Journal of Geodynamics 45 (2008) 133–145
JOURNAL OF GEODYNAMICS
http://www.elsevier.com/locate/jog

Pattern of recent vertical crustal movements in Canada

Azadeh Koohzare *, Petr Vaníček, Marcelo Santos
Department of Geodesy and Geomatics Engineering, University of New Brunswick, P.O. Box 4400, Fredericton, NB, Canada E3B 5A3

Received 19 February 2007; received in revised form 30 July 2007; accepted 12 August 2007

Abstract

We used the method of smooth piecewise algebraic approximation to automatically compute a smooth approximation of large functional scattered re-levelling data and historical tide gauge records given over Canada and northern US to thereby compile a unified map of vertical crustal movements (VCM). The area of study is divided into pieces and piecewise algebraic surfaces are fitted to the tide gauge trends and to the height difference differences, computed from monthly mean sea-level and re-levelling segments, respectively. When the surfaces are fitted to the data, a set of continuity and smoothness constraints is imposed in such a way that rather than the surfaces being fitted sequentially, they are fitted simultaneously, using the constraints as a set-conditions which the parameters of the surfaces must also satisfy.

The VCM model obtained in this research gives enough details of the movements. It highlights the long wavelength spatial and temporal variations of the crust in Canada, mainly due to postglacial rebound (PGR). In Eastern Canada, the PGR hinge line appears from Gulf of St. Lawrence in the map of VCM. It follows the Atlantic coast line to the south of the country. In the Great Lakes, the relative movements or the tilt varies slightly between 0.5 and 1.5 mm/year per hundred kilometers) along northeast–southeast direction, which is toward the maximum ice center in Hudson Bay. The computed tilt is in a relatively good agreement with the tilt obtained from the glacial isostatic adjustment (GIA) model of ICE-3G (VM2) in this region ($\sim$1 mm/year per hundred kilometers). The predicted rate of tilt in eastern prairies in Manitoba from VCM is in the range of 1.5–2 mm/year per hundred kilometers toward Hudson Bay. This solution is in good agreement with the results of previous studies for subsidence in southern Lake Athabaska in Saskatchewan and for uplift in southern prairies. However, GIA models do not agree with such findings. The zero line in the map of VCM nearly follows the Pacific coastal line, which is consistent with the PGR zero line in the prairies.

Keywords: Vertical crustal movements; Levelling; Tide gauges; Temporal crustal variations; Glacial isostatic adjustment

1. Introduction

It has been recognized for several decades that the determination of vertical crustal movements (VCM) using geodetic observations is of high importance in geosciences. In geophysics, for example, VCM is of primary interest in the study of the rheology of the mantle and lithosphere, which is crucial in understanding geodynamical processes (for recent reviews, see Peltier, 1998; Lambert et al., 2001; Wahr et al., 1995). In geodesy, they are important in the definition of vertical datum that is required in many application areas such as navigation, mapping, and environmental studies (see for instance Rapp, 1994; Pan and Sjöberg, 1998; Henton et al., 2006).

There are different kinds of geodetic data with vastly different accuracies, which contain information on the vertical movements of the crust. As such, one problem is to put together the various types of available data with VCM models designed to detect and describe the crustal movements.

During the past few decades, intensive research and progress have been made on the development of vertical crustal deformation models. Very comprehensive reviews of modeling strategies for vertical crustal deformation are presented by e.g. Vaníček and Christodulids (1974), Holdahl and Hardy (1978), Chrzanowski et al. (1986), Vaníček and Sjöberg (1987), Carrera et al. (1991), Liu and Parm (1996), and Liu and Chen (1998). All of the models can estimate deformation parameters for multi-epoch observations. They provide the convenience of predicting deformation in time–space domains, which is very important for studying the time and areal distribution of deformation (Liu and Chen, 1998). However, some of the above models have limitations in data fitting. Other limitations of the crustal deformation mod-

* Corresponding author. Fax: +1 506 453 4943.
E-mail address: a.koohzare@unb.ca (A. Koohzare).

0264-3707/$ – see front matter. Crown Copyright © 2007 Published by Elsevier Ltd. All rights reserved.
doi:10.1016/j.jog.2007.08.001

els include severe restrictions on the number and distribution of data. There are also limitations to handle large linear equation systems. Some of the crustal motion models even cannot be used for different types of data, point values and relative values (tilt) between points. In addition, the above models cannot be used in their current form over wide areas of interest such as Canada where different geophysical phenomena contributes to the deformation. Crustal deformation in Canada is a complex process and should be analyzed by choosing different models for different deformation areas of interest. However, selecting a particular deformation model for a particular deformation area is very difficult. Therefore, this contributes additional limitation to the use of the previous models of crustal motions in Canada.

The first VCM model which covered the whole of Canada was compiled by Vaníček and Nagy (1981) using precise re-levelled segments and tide gauge records. The country was divided into regions and polynomial surfaces of order 2, 3 and 4 were calculated by the method of least squares for each region to obtain representations of the vertical movements. A considerably larger database has been gathered since then, and this, together with additional insight into the nature of the data, led to the recompilation of the map of VCM of Canada by Carrera et al. (1991) in which a polynomial surface was fitted to the data. Those models also had some limitations. The main limitation is that to get the details needed for the map to be meaningful, the order of the velocity surface would have to be too high. This would cause wild oscillations (artifacts) where there is no data.

In this work, we compiled a numerically manageable VCM from scattered re-levelling data and tide gauge records in Canada by dividing the area of interest into patches and fitting a piecewise surface to 2D observation points and tilt between them. When the surfaces are fitted to the data, the sets of continuity and smoothness constraints were imposed in such a way that the surfaces are fitted simultaneously.

The VCM model should be also physically meaningful so that it not only describes the actual movements of the crust, but also opens doors to the study of the causes of the movements, validates the geophysical models of the movements and perhaps, as an independent constraint, resolves the trade-off in some of the geophysical models (Velicogna and Wahr, 2002). In order to investigate whether the compiled surface is physically meaningful, it is required to study different geodynamical processes that contribute to the deformation of the crust and the interaction between them, and to find the best approach to reconcile geodetic data with geophysical phenomena.

The main contribution of this paper is to present the most recent pattern of VCM in Canada, compare it with previous studies in the region and to physically interpret the results in different regions in Canada.

2. Data, error analysis and treatment

The data used as inputs for the VCM model are of two kinds: re-levelling information from the first-order levelling network, and sea-level records. Other data, such as rate of gravity changes or $\dot{g}$, geodetic height changes or $\dot{h}$, location of tectonic boundaries, seismicity information, etc., are added in the database for further analysis and interpretations of the results.

Table 1
Number of re-levelled segments in Canada used in this study

Province	Number of first-order re-levelling data
Alberta (AB)	1,498
British Columbia (BC)	10,826
Manitoba (MB)	2,213
New Brunswick (NB)	1,294
Newfoundland (NF)	513
Northern Territories (NT)	492
Nova Scotia (NS)	2,336
Ontario (ON)	15,249
Prince Edward Island (PEI)	63
Quebec (QC)	10,127
Saskatchewan (SK)	1,681
Yukon (YK)	48
Total	46,340

The Canadian first-order levelling database was provided to us by Geodetic Survey Division (GSD), Natural Resources Canada, in a format that the data could be categorized by provinces. These covered the period 1909–2003 and spanned from less than 500 m to several tens of kilometers. The re-levelled segments were pre-processed to eliminate the ones that showed unreasonable local tilts. The quality control criterion applied to the re-levelled segments was implemented by means of rejection criterion for height difference differences per distance in time, greater than 0.1 mm/(km year^{-1}). By applying this threshold, 1882 Canadian re-levelled segments were eliminated. In any case, most of the eliminated re-levelled segments would have been eliminated anyways because they were too short to contribute to the analysis. Table 1 shows the number of extracted re-levelled data in each province in Canada.

The Canadian sea-level information includes monthly mean sea and lake level values which were provided by Marine Environmental Data Service (MEDS), and the US monthly mean sea-level records were downloaded from the NOAA website.[1] The apparent sea-level rise left after removal of the global eustatic signal is assumed to represent a vertical motion of the crust of the same magnitude but of opposite sign.[2] The assumed global eustatic sea-level rise in this study is the value of 1.8 mm/year from Douglas et al. (2001).

The analysis of the tide gauge records was based on monthly averaged sea-level data collected at tide gauge stations, since it is a known fact that averaging sea-level data over a month acts as an effective filter of high frequency oceanic signals (Godin, 1972; Cartwright, 1983).

Typically, monthly averages of sea level oscillate within the range of about 0.5 m throughout years of observations. Since the linear trend of interest is a fraction of a cm/year, it is important to have records as long as possible. In the studies of vertical

[1] http://tidesandcurrents.noaa.gov/station_retrieve.shtml?type=Historic+Tide+Data.

[2] The vertical crustal motion is the movement of the crust relative to geoid or mean sea level, and the isostatic relative sea level changes is referred to the position and height of sea relative to the land.

Table 2
Sea-level linear trends and their standard deviations of the tide gauges in Canada and Northern US in mm/year

Code	Tide gauge	Location latitude (°N)/ longitude (°W)	Velocity based on differencing (mm/year) from Carrera et al. (1991).[a]	Data available for this study	Point velocity (mm/year)	Velocity based on differencing (mm/year) in this study
1	Halifax, NS	44°39′.6/63°35′.4	3.56 ± 0.08	1919–2003	3.27 ± 0.05	3.27 ± 0.05
2	North Sydney, NS	46°13′.2/60°15′.0	3.87 ± 0.46	1970–2003	3.07 ± 0.54	3.42 ± 0.37
3	Yarmouth, NS	43°50′.4/66°07′.2	4.75 ± 0.35	1900–2003	2.85 ± 0.15	4.17 ± 0.18
4	Point Tupper, NS	45°06′.0/61°22′.2	4.31 ± 0.79	1971–1992	1.67 ± 0.70	3.12 ± 0.80
5	Pictou, NS	45°40′.8/62°42′.0	3.68 ± 0.33	1957–1996	2.30 ± 0.35	3.70 ± 0.21
6	Boutilier Point, NS	44°39′.6/63°57′.6	3.97 ± 0.49	1970–1983	3.00 ± 1.40	
7	Charlottetown, PEI	46°13′.8/63°07′.2	3.55 ± 0.11	1905–2003	3.21 ± 0.08	3.30 ± 0.09
8	Rustico, PEI	46°28′.2/63°16′.8	3.28 ± 0.47	1972–1996	3.92 ± 0.68	3.92 ± 0.68
9	Saint Jonh, NB	45°16′.2/66°03′.6	3.01 ± 0.14	1905–2003	2.50 ± 0.11	–
10	Shediac Bay, NB	46°15′.0/64°31′.8	–	1971–1992	1.23 ± 0.70	2.50 ± 0.14
11	Lower Escuminac, NB	47°04′.8/64°53′.4	2.12 ± 0.48	1973–2003	1.98 ± 0.66	2.10 ± 0.31
12	St. Johns, NF	47°33′.6/52°42′.6	1.93 ± 0.36	1935–2003	2.10 ± 0.25	–
13	Argentia, NF	47°18′.0/53°58′.8	–	1971–2003	1.70 ± 0.50	–
14	Harrington Harbour, NF	50°28′.8/59°28′.2	0.13 ± 0.16	1939–1989	−0.72 ± 0.17	–
15	Rivière au Renard, QC	48°58′.8/64°22′.2	−0.32 ± 0.77	1969–2003	−0.49 ± 0.16	−0.32 ± 0.15
16	Rimouski, QC	48°28′.8/68°31′.2	–	1984–2003	−0.24 ± 0.90	
17	Sept Illes, QC	50°10′.8/66°22′.2	1.87 ± 0.41	1972–2003	2.01 ± 0.25	0.19 ± 0.11
18	Point au Père, QC	48°31′.2/68°28′.2	−0.10 ± 0.16	1900–2003	−0.31 ± 0.07	−0.31 ± 0.07
19	Quebec, QC	46°49′.8/71°10′.2	1.05 ± 0.28	1900–2003	−0.52 ± 0.16	
20	Baie Comeau, QC	49°13′.8/68°07′.8	−0.62 ± 0.47	1964–1991	−5.77 ± 0.72	−0.62 ± 0.31
21	Tadoussac, QC	48°08′.4/69°42′.6	−1.21 ± 0.80	1966–1995	−5.08 ± 0.62	−1.21 ± 0.21
22	St. Francois, QC	47°00′.0/70°48′.6	1.70 ± 0.28	1962–2003	−0.48 ± 0.45	
23	St. Jean Port Joli, QC	47°13′.2/70°16′.8	−0.88 ± 1. 65	1968–1980	−5.38 ± 2.18	−0.88 ± 1. 64
24	St. Anne des Monts, QC	49°07′.2/66°28′.8	−0.55 ± 0.60	1967–1997	−0.89 ± 0.44	−0.40 ± 0.49
25	Bar Harbour, ME[b]	44°23′.5/68°12′.3	–	1947–1999	2.18 ± 0.16	–
26	Eastport, ME	44°54′.2/66°59′.1	–	1929–1999	2.21 ± 0.13	–
27	Portland, ME	43°43′.8/70°12′.4	–	1912–1999	1.91 ± 0.09	–
28	Seavey Island, ME	43°05′.0/70°44′.0	–	1926–1999	1.75 ± 0.17	–
29	Tofino, BC	49°09′.0/125°54′.6	−1.04 ± 0.70	1909–2002	−1.55 ± 0.16	−1.55 ± 0.16
30	Port Alberni, BC	49°13′.0/124°48′.6	+3.07 ± 0.60	1970–1997	−0.01 ± 0.78	−0.37 ± 0.32
31	Bamfield, BC	48°49′.8/125°07′.8	+1.05 ± 0.46	1970–2002	+0.37 ± 0.62	+0.92 ± 0.19
32	Port Renfrew, BC	48°33′.0/124°25′.2	+0.24 ± 0.56	1957–1997	+1.24 ± 0.69	+1.57 ± 0.36
33	Sooke, BC	48°22′.2/123°43′.2	−0.30 ± 0.39	1958–1985	+1.95 ± 1.41	+0.82 ± 0.52
34	Victoria, BC	48°25′.2/123°22′.2	+0.74 ± 0.10	1925–2002	+0.08 ± 0.36	+0.73 ± 0.14
35	Patricia Bay, BC	48°39′.0/123°27′.0	+0.66 ± 0.48	1966–2002	−0.31 ± 0.69	+1.01 ± 0.19
36	Fulford Harbor, BC	48°46′.2/123°27′.0	+0.20 ± 0.13	1952–1992	+0.16 ± 0.35	+0.24 ± 0.36
37	Stevenson, BC	49°07′.2/123°10′.8	+1.75 ± 0.38	1969–1997	+2.10 ± 0.60	+1.27 ± 0.39
38	Vancouver, BC	49°17′.4/123°06′.6	+0.24 ± 0.10	1909–2002	+0.30 ± 0.10	+0.30 ± 0.10
39	Point Atkinson, BC	49°20′.4/123°15′.0	+0.93 ± 0.11	1914–2002	+0.85 ± 0.12	+0.80 ± 0.10
40	Campbell River, BC	50°01′.2/125°13′.8	+0.09 ± 0.23	1958–2003	−2.00 ± 0.51	−1.58 ± 0.20
41	Alert Bay, BC	50°34′.8/126°55′.8	−1.06 ± 0.22	1948–1979	−1.62 ± 0.62	−1.22 ± 0.63
42	Port Hardy, BC	50°43′.2/127°29′.4	+0.56 ± 0.38	1964–2002	−1.06 ± 0.44	−0.65 ± 0.21
43	Bella Bella, BC	52°09′.6/128°08′.4	+1.92 ± 0.46	1906–2002	−0.34 ± 0.31	−0.89 ± 0.19
44	Queen Charlotte City, BC	53°15′.0/132°04′.2	+1.28 ± 0.54	1957–2002	−0.88 ± 0.34	−0.88 ± 0.34
45	Prince Rupert, BC	54°19′.2/130°19′.2	+3.32 ± 0.53	1909–2002	+1.04 ± 0.14	+1.04 ± 0.14
46	Friday Harbor, WA	48°33′.0/123°00′.6	+0.63+0.12	1934–1999	+1.24 ± 0.20	+1.07 ± 0.19
47	Toke Point, WA	46°42′.6/123°57′.9	–	1973–1999	+2.82 ± 1.05	+1.20 ± 0.47
48	South Beach, OR	44°37′.2/124°02′.5	–	1967–1999	+3.51 ± 0.73	+2.34 ± 0.54
49	Seattle, WA	47°36′.3/122°20′.4	+1.98+0.13	1898–1999	+2.11 ± 0.10	+2.11 ± 0.10
50	Port Townsend, WA	48°06′.6/122°45′.6	–	1972–1999	+2.82 ± 0.88	+2.13 ± 0.12
51	Port Angeles, WA	48°07′.5/123°26′.4	–	1975–1999	+1.49 ± 1.10	+0.37 ± 0.17
52	Neah Bay, WA	48°22′.2/124°37′.2	–	1934–1999	−1.41 ± 0.22	−1.41 ± 0.22
53	Charleston, OR	43°20′.7/124°19′.2	–	1970–1999	+1.74 ± 0.87	+0.48 ± 0.55
54	Astoria, OR	46°36′.3/123°46′.2	–	1925–1999	−0.16 ± 0.24	−0.16 ± 0.34
55	Cherry Point, WA	48°51′.6/122°45′.6	–	1973−1999	+1.39 ± 0.94	−0.03 ± 0.14

[a] The signs are different from the original technical report due to different definitions.
[b] Tide gauges in the USA had their values taken from http://www.coops.nos.noaa.gov/sltrends/sltrends.html.

crustal motions, tide gauge records with longer time spans are more reliable. Sea-level records with duration of a few tens of years may not be taken as representative for the secular trends sought, if they are studied individually. However, when they are treated in a differenced mode, the secular variations can be accurately estimated (Koohzare et al., 2006b; Vaníček and Carrera, 1993). In this study the differencing method is used to treat the records of those adjacent tide gauges that are correlated. Therefore, the subset of sites is selected to include all stations for which continuous records of at least 10 years duration are available. The importance of applying this selection criterion is a consequence of the strength of the inter-annual variability, which must be averaged over if the secular variations are to be accurately estimated. Table 2 lists the linear trends of the tide gauges in Canada and northern US considered for this study and compare them with the results published in Carrera et al. (1991). Small differences between the results shown in Table 2 were expected because this study incorporated data collected in the past 15 years since the previous study. In addition, there are some tide gauges whose records were not considered in the compilation of VCM in the previous work mainly because of the shortness of the data series or probable systematic errors reported in Carrera et al. (1991). For example, the records of Shediac Bay was reported to be contaminated by systematic errors (Carrera et al., 1991), however, longer records of this tide gauges does not show such error, and its records were incorporated in this study.

The distribution of re-levelling segments and the location of tide gauges and lake gauges are depicted in Fig. 1.

3. Compilation of a map of VCM in Canada

The procedure of fitting a surface to the geodetic data involves the use of both the point rates and the gradients simultaneously, together with their proper weights. The point rates are determined from some of the tide gauge data which were selected to be used in the point velocity mode, and the gradients come from re-levelled segments and tide gauge pairs. Assuming the velocity to be constant in time, the difference of the two levelled height differences divided by the time span between the two levellings gives the velocity difference between the two levelling segment ends.

In general, if we divide the area of study into p patches, the resulting function is a polynomial function of degree n with p patches. A given polynomial in the mth ($m = 1, 2, \ldots, p$) patch looks as follows:

$$V_m(x, y) = \sum_{i=0}^{n_x} \sum_{j=0}^{n_y} c_{ij,m}(x - x_{0m})^i (y - y_{0m})^j. \tag{1}$$

where V_m is the algebraic least squares velocity surface for patch m, fitted to the desired data (x, y). The pair (x_{0m}, y_{0m}) represents the position of the origin of the coordinate system in patch m and $c_{ij,m}$ are the unknown coefficients in patch m. n_x and n_y are

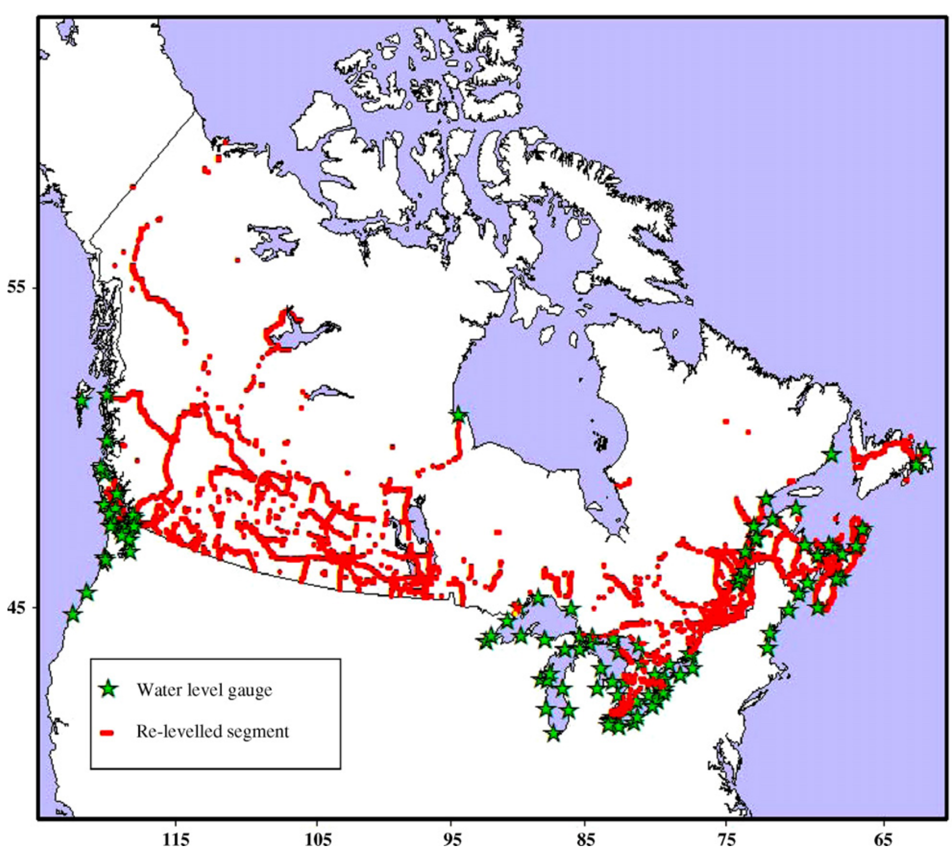

Fig. 1. Data distribution used in the computations. Red dot lines show relevelled segments. Stars indicate the location of water level gauges. (For interpretation of the references to colour in this figure legend, the reader is referred to the web version of the article.)

the degrees of polynomials along x and y directions, respectively.

If m and m' represent the two adjacent patches having common border mm', then in order to piece the polynomials together, the following conditions should be satisfied:

$$V_m(x_{mm',k}, y_{mm',k}) = V_{m'}(x_{mm',k}, y_{mm',k}) \quad \forall k = 1, 2, \ldots, q; \tag{2.a}$$

$$\left.\frac{\partial V_m(x, y)}{\partial x}\right|_{\substack{x = x_{mm',k}\\ y = y_{mm',k}}} = \left.\frac{\partial V_{m'}(x, y)}{\partial x}\right|_{\substack{x = x_{mm',k}\\ y = y_{mm',k}}} \quad \forall k = 1, 2, \ldots, q; \tag{2.b}$$

$$\left.\frac{\partial V_m(x, y)}{\partial y}\right|_{\substack{x = x_{mm',k}\\ y = y_{mm',k}}} = \left.\frac{\partial V_{m'}(x, y)}{\partial y}\right|_{\substack{x = x_{mm',k}\\ y = y_{mm',k}}} \quad \forall k = 1, 2, \ldots, q. \tag{2.c}$$

$(x_{mm',k}, y_{mm',k})$ is the position of kth nodal point in the border mm' joining patches m and m'.

Here, q represents the maximum number of the nodal points in the common border between patch m and patch m'.

Conditions (2.a) make sure that the piecewise polynomial fits to the nodal points ($P\ mm'$, 1, $P\ mm'$, 2, ..., $P\ mm'$, $k = q$) located in the predefined border mm' between two patches m and m'. These conditions imply that the surface is continuous everywhere in the region. Conditions (2.b) and (2.c) ensure that the polynomials are continuous in slope along x and y directions, respectively. The main mathematical model is given by Eq. (1) while all the conditions under (2) constitute the constraints on the main model. The least square solutions are then found using Lagrange identifier (Koohzare, 2007).

The predicated error (posteriori standard deviation) of the velocity surface is derived from the covariance matrix of the computed coefficients. Before this is done, the coefficients are filtered statistically on a pre-selected significance level. The filtering is done in the orthogonal solution space, applying the Gram–Schmit's orthogonalization, and de-orthogonalized back into natural solution space.

In this study, it was decided to divide the area of study into some square and rectangular patches with different sizes in which the border between two adjacent patches is always a straight line parallel to the coordinate axis. Therefore, the region of study, Canada, was divided into patches of different sizes depending on the number and the distribution of data. The size of the patches was initially selected to be $2^\circ \times 2^\circ$ and if there were not enough data in a particular patch, or the data were not well distributed, the adjacent patches were combined to create a bigger patch.

The appropriate degree of the velocity surface is determined by testing the 'a posteriori variance factor'. This is computed from

$$\hat{\sigma}_0^2 = \frac{\hat{\mathbf{r}}^T \mathbf{C}_l^{-1} \hat{\mathbf{r}}}{\nu}, \tag{3}$$

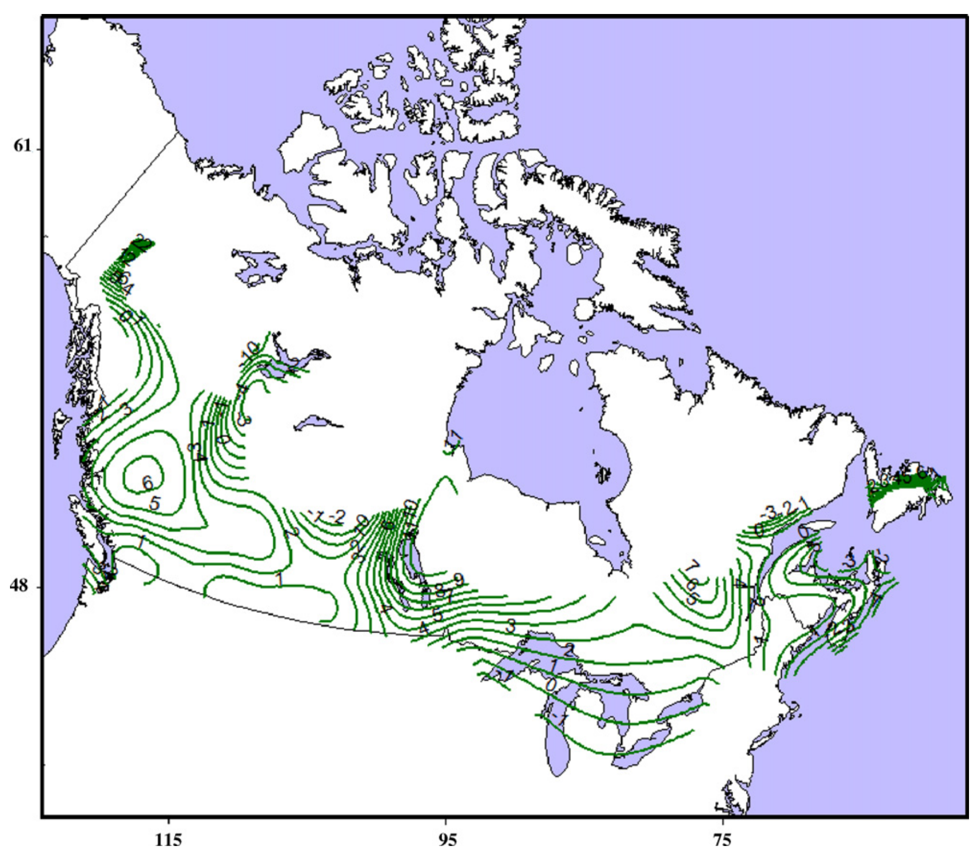

Fig. 2. Pattern of vertical crustal movements in Canada using SPAA, in mm/year.

where $\hat{\boldsymbol{r}}$ is the vector of least squares estimations of residuals and ν denotes the number of degrees of freedom. All degrees of the polynomials yielded the a posteriori variance factors between 5 and 9. The value of $n=3$, degree of polynomial, was finally selected as the highest degree compatible with data distribution in most of the patches.

One frequent problem in VCM modeling using SPAA is that the system of normal equations might be ill-conditioned in the areas with poor distribution of data. This means that the solution is hypersensitive to changes in the position of data. One remedy is to combine the patch with poor distribution of data with adjacent patch or patches, to create a patch with a more reasonable distribution of data. In order to secure a numerically stable solution, the origin of the coordinate system should also be chosen carefully. It was decided to choose the origin of the coordinate system of each patch either in the center of that patch itself or in the center of the mass point of the patch, depending on which leads to smaller standard deviation for the absolute term of the VCM surface.

Fig. 2 shows the contour map of VCM in Canada; and the map of standard deviation of the computed VCM is depicted in Fig. 3. The final map is the production of 33 patches, and cubic polynomials (Koohzare, 2007). A hypsometric map of VCM in Canada, which is confined with the distribution of data in the area are illustrated in Fig. 4.

The method of SPAA avoids many of the limitations associated with traditional approaches of data fitting such as the requirement that the data be of point values, as it is seen in MQ method (Holdahl and Hardy, 1978) and in B-splines (Gregorski et al., 2000; Greiner and Hormann, 1996); or that they should be on grid or at least well distributed (Zhou et al., 1997). SPAA is not restricted to low degree polynomial (as it is seen in Carrera et al., 1991; Vaníček and Nagy, 1981) and the smoothness of the resulting function is guaranteed along the patch boundaries by imposing the continuity and smoothness (zero and first derivative) constraints and the degree of smoothness can be simply controlled by the number and degree of differentiability constraints in the model, which results in a smooth surface. However, this model should be used with certain caution, as imposing too many constraints results in excessive stiffening of the surface.

4. Discussion and physical interpretation of the results in each region in Canada

There are different geophysical phenomena responsible for the crustal deformation in Canada. These can be global, regional or local phenomenon. In this section, the computed deformations from VCM in different regions in Canada are interpreted where it is possible.

4.1. Eastern Canada

During the last ice age (late Pleistocene), ice advanced over the St. Lawrence valley and extended east into the Maritime

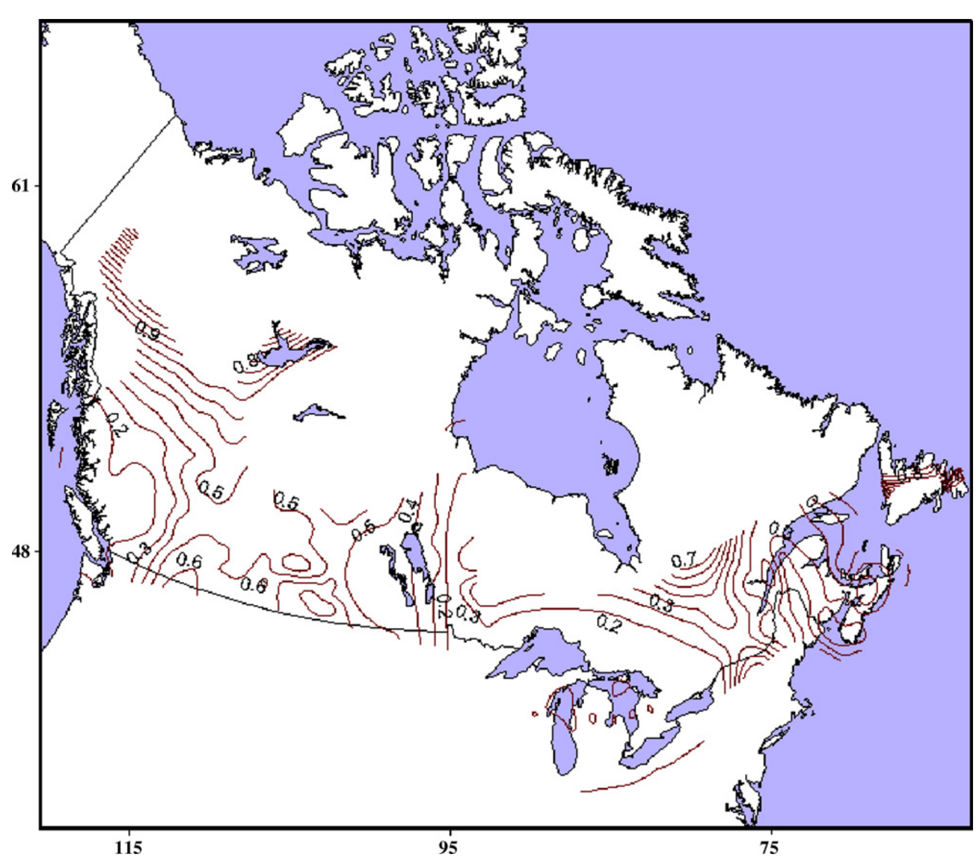

Fig. 3. Pattern of the standard deviation of the predicated vertical crustal movements in Canada using SPAA, in mm/year.

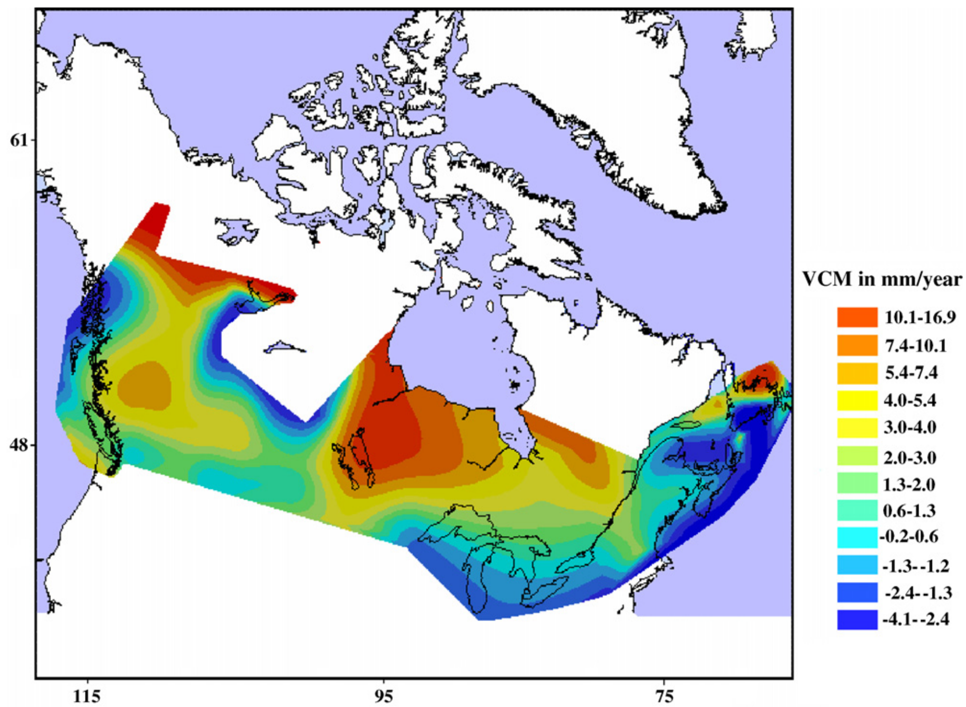

Fig. 4. A color map of vertical crustal movements in Canada using SPAA.

Provinces and south into New England (Dyke, 2004). The weight of the ice depressed the surface of the Earth and flow in the fluid mantle created a peripheral bulge outside the glaciated region. Upon thinning and melting the ice sheet, the lithosphere began to rebound toward its former position of isostatic equilibrium and the peripheral bulge began to collapse and perhaps migrate toward the center of uplift. Some GIA models indicate that the hinge line between uplift to the north and subsidence to the south is near the St. Lawrence valley (e.g., Tushingham and Peltier, 1991; Peltier, 2002). These first-order features of PGR-related crustal deformation are confirmed by various geodetic measurements in central and eastern North America (e.g., Lambert et al., 2001; Park et al., 2002; Sella et al., 2002; Koohzare et al., 2006a). Therefore the subsidence in Maritimes, predominantly in Nova Scotia and eastern New Brunswick seen in the VCM compiled in this study is due to postglacial rebound. The map of VCM in this area which depicts this phenomenon is shown in Fig. 5.

In Eastern Canada, there are also areas of substantial seismicity and earthquake hazard. The St. Lawrence valley, eastern Quebec (Fig. 6), is one of the most seismically active regions of eastern North America (Lemieux et al., 2003; Mazzoti et

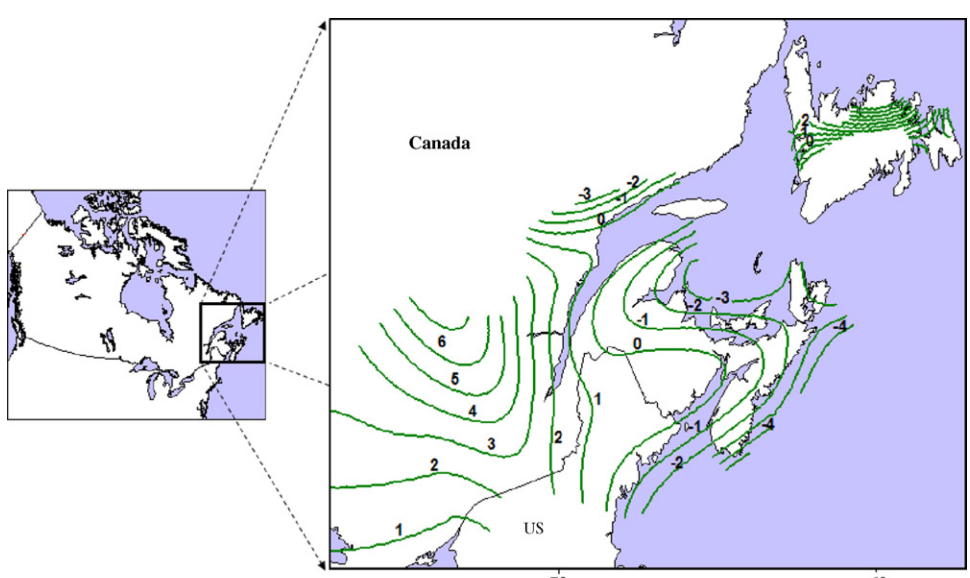

Fig. 5. The contour map of VCM in Eastern Canada. The contours are in mm/year.

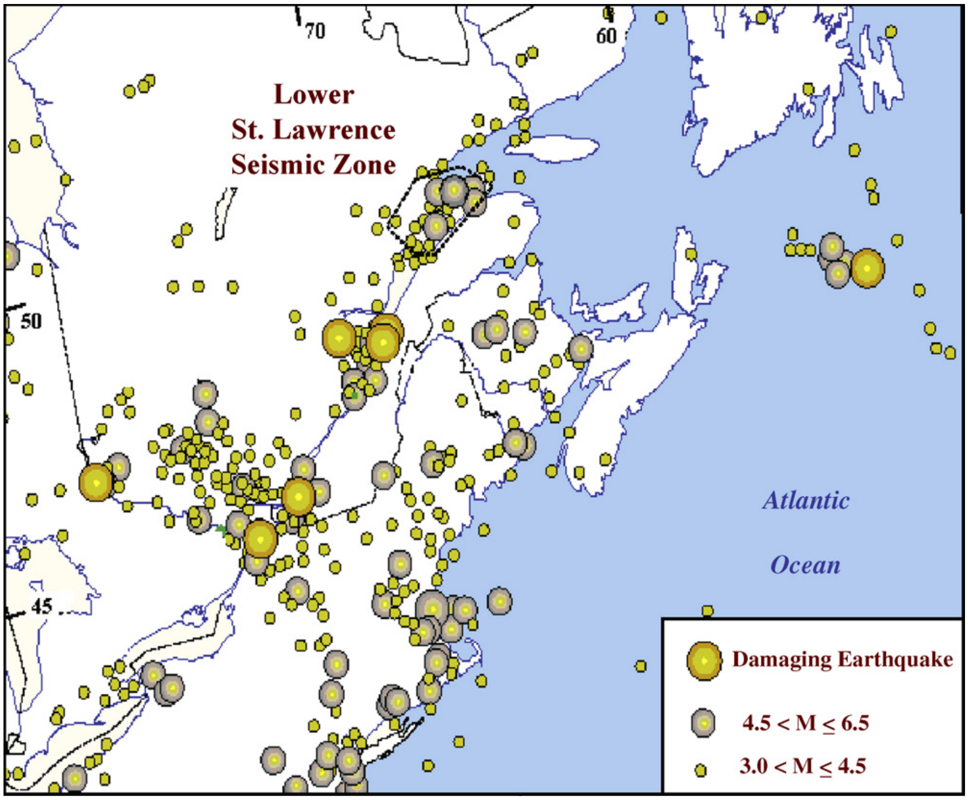

Fig. 6. Seismicity map of Eastern Canada with location of the Lower St. Lawrence seismic zone (LSZ) (Lamontagne et al., 2003).

al., 2005). This area has a large range of intraplate earthquake patterns, from zones with large ($M = 6$–7) earthquakes to zones with very little background seismicity (e.g., Adams and Basham, 1991). The driving mechanism behind these earthquakes is difficult to be determined as due to the fact that the seismic activities are not directly correlated with plate interactions in this region. About 100 km downriver from Quebec City, the Charlevoix seismic zone (CSZ) is the strongest locus, with numerous small to medium earthquakes as well as five $M > 6$ events in the last 350 years. In contrast, the area between Quebec City and Montreal shows very little seismic activity. Another seismic zone in Eastern Canada is Lower St. Lawrence seismic zone. The St. Lawrence valley is characterized by large eastward dipping normal faults with up to a few kilometers of motion documented in the Precambrian basement (Kumarapeli, 1985). The normal fault system is capped by westward verging thrust faults and napes of the Appalachian orogen. This Paleozoic cover is only a few kilometers thick in most of the St. Lawrence region.

A meteorite impact (350 Ma) in the southern part of the Charlevoix seismic region contributed additional complexity by creating a 60 km diameter system of concentric faults and fractures (Randot, 1968; Lemieux et al., 2003).

Although the VCM do not discriminate between various models of crustal deformation, it provides important constraints on GIA models, and large earthquake recurrence.

The PGR hinge line appears from the island of Newfoundland and Gulf of St. Lawrence in the map of VCM. It follows the Atlantic coast line to the south of the country (see Fig. 5). This gives some information about deglaciation history of ice model. From $\dot{g}$ maps (Pagiatakis and Salib, 2003), the PGR hinge line starts from the same region and follows roughly the Canadian East coast, along Labrador Sea and Buffin Island. The rate of geodetic height changes in Maritimes from Canadian Base Network (CBN) solution[3] and Sella et al. (2007) are also consistent with our results. The only difference is that the probable PGR hinge line is parallel to the St. Lawrence River in both GPS solutions, while in VCM map, the PGR hinge line follows the coast line. It should be noted that the GPS solution gives the rate of height changes with respect to a reference ellipsoid. The difference between $\dot{H}$ and $\dot{h}$, theoretically, reflects the temporal variations of the geoid (see Fig. 7).

The pattern of $\dot{H}$ shown in the north eastern margin of the former Laurentide ice sheet (the border of which has been postulated to have been parallel to St. Lawrence River) is complicated due to the probable fragmentation of the crust in this zone. The earlier reported uplift of the northern New Brunswick and the subsidence of the South St. Lawrence River (Vaníček, 1976; Carrera and Vaníček, 1994) are here more sharply defined.

Another interesting feature derived from the VCM is a ridge of uplift across the St. Lawrence River, following the Hudson River path in US. The peak is in Charlevoix and might

[3] The solution was provided to us by Dr. Mike Craymer, Geodetic Survey Division, Natural Resources Canada 2006, which was used in Sella et al. (2007) solution. Throughout this paper, the GSD solution in CBN stations is called the CBN solution.

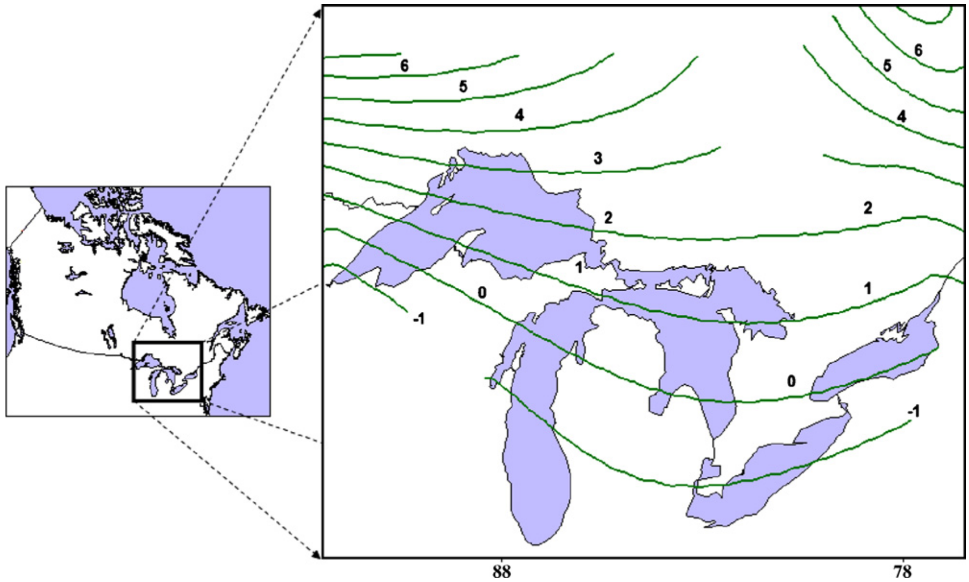

Fig. 7. The contour map of VCM in the Great Lakes. The contours are in mm/year.

correspond to the seismic vertical strains, but it needs more investigations.

4.2. Great Lakes

Due to PGR, while the land north of the Great Lakes is rising, that south of the Great Lakes is subsiding to maintain equilibrium. Hence, residents on the south shores of the Great Lakes have noticed water level rising slowly over time, while those on the north shores have noticed declining water levels.

The location of postglacial rebound hinge line derived from the VCM map passes through the Great Lakes and is close to the location of zero line from GIA models, more closely to the GIA adopting ICE-3G ice history and the standard Earth model (Tushingham and Peltier, 1991).

Since the VCM is the result of simultaneous solution over the whole Canada, the absolute value for the vertical movements in the Great Lakes is obtained from all the tide gauges which are used in the computation; however, the linear trend of the Churchill tide gauge in Hudson Bay, being the closest tide gauge to the Great Lakes controls the absolute term of the VCM in this area more than other tide gauge records.

The relative movements or the tilt in this area varies slightly between 0.5 and 1.5 mm/year per hundred kilometers along northeast–southeast direction, which is toward the maximum ice center in Hudson Bay. The computed tilt is in a relatively good agreement with the tilt obtained from the GIA model of ICE-3G (Tushingham and Peltier, 1991) in this region (∼1 mm/year per hundred kilometers). The present-day tilting of the Great Lakes from our VCM is consistent with the tilting based on the analysis of water level gauges in the area (Mainville and Craymer, 2005; Coordinating Committee on Great Lakes Basic Hydraulic and Hydrologic Data, 1977). The VCM in this area is also in good agreement with the maps of $\dot{h}$ (CBN solution and Sella et al., 2007) and $\dot{g}$ (Pagiatakis and Salib, 2003).

4.3. Eastern prairies

The predicted rate of tilt in eastern prairies (Manitoba) from VCM is in the range of 1.5–2 mm/year per hundred kilometers toward Hudson Bay (see Fig. 8). This is significantly larger than the predicted tilt from GIA models using standard ICE and Earth models (∼1 mm/year per hundred kilometers in Manitoba). However, it should be noted that due to the poor distribution of relative sea level compared to the distribution of Laurentide ice, GIA models in this area are uncertain. The difference between the predicted present-day crustal uplift rate for two models, ICE-3G (Tushingham and Peltier, 1991) and ICE-4G (Peltier, 1994) reaches to 1.5 mm/year in this area (Lambert et al., 1998).

The relative vertical displacement of pro-postglacial lake strand line has been the principal geological observable used to quantify past postglacial rebound in this region. Using the tilting of the 9.5 kyr before present. Campbell strand line south and west of Lake Winnipeg and the rate of decreasing in absolute gravity values measured from 1987 to 1995 at Churchill, and also the present-day regional tilt rate derived from water-level gauges in southern Manitoba lakes, Lambert et al. (1998) has indicated the ‘disagreement’ of all these data types in Manitoba with ICE-3G and the ‘standard’ Earth model. Therefore, the map of VCM in this area plays an important role in the proper modifications of the uncertain parameters in the models, in such a way that a better fit with VCM is obtained. Either a further modification in the ice-sheet east of Manitoba or a thinner lithosphere (as recommended by Wolf, 1985 and Tackmam, 1997), or both, may be required to solve the disagreement. The uplift around northern Winnipeg Lake seen in the map of VCM and the negative values for the $\dot{g}$ (Pagiatakis and Salib, 2003) in the same

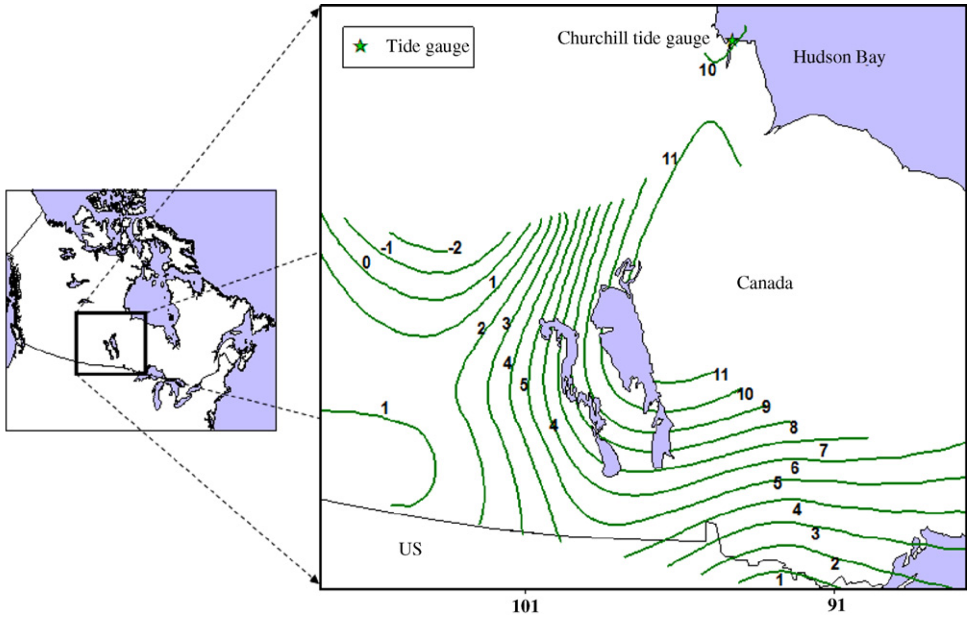

Fig. 8. The contour map of VCM in Manitoba. The contours are in mm/year. Star shows the location of tide gauge.

area are consistent. There is also a good agreement between the maps of VCM and the rate of geodetic height changes in CBN stations.

4.4. Western and central prairies

The VCM map in western and central prairies is shown in Fig. 9. An interesting feature seen from this map is the subsidence in southern Lake Athabaska in Saskatchewan. While this is in good agreement with previous map of VCM (Carrera et al., 1991), GIA models and the pattern of geodetic height changes do not show such local subsidence. It is expected that the subsidence is due to some local movements in the area. In southern prairies, uplift is seen. It might roughly corresponds with the location of the prairie evaporate, a 100 m thick salt layer (Jim Merriam, personal communications). This load causes local subsidence of the region. Distinction between different geophysical causes which are responsible for such movement, local load effect, PGR or both, needs further investigations.

4.5. British Columbia and Pacific coast

The zero line in the VCM map loops around the Saskatchewan subsidence area, and creates an uplift dome like area in British Columbia (BC) (see Fig. 10). This uplift is, partly, due to the

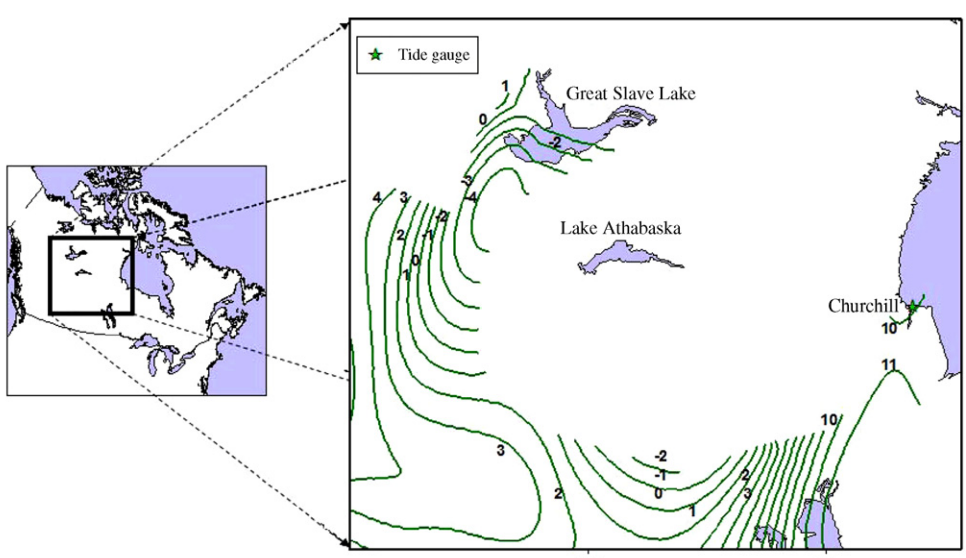

Fig. 9. The contour map of VCM in southern and western prairies. The contours are in mm/year.

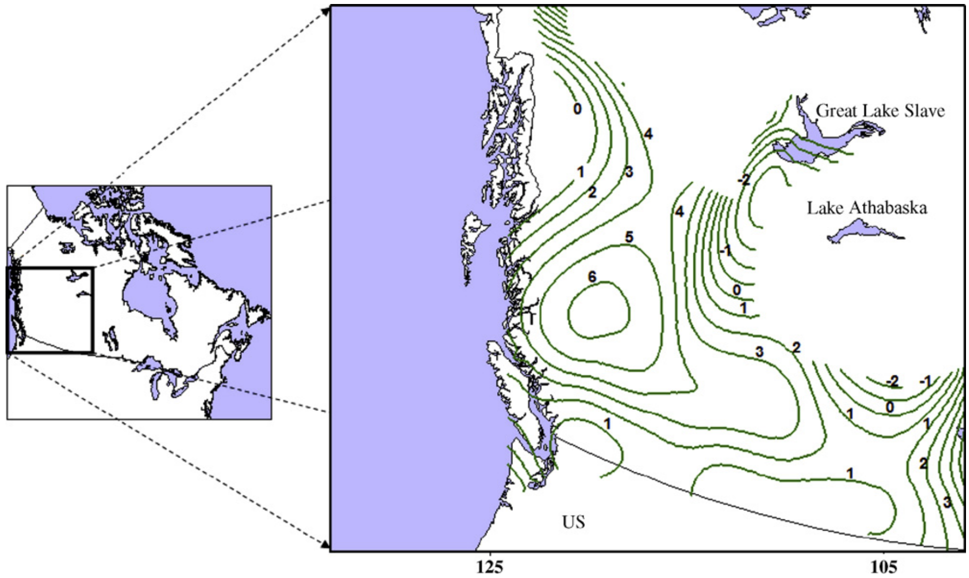

Fig. 10. The contour map of VCM in British Columbia. The contours are in mm/year.

PGR, and is consistent with GIA models of Tushingham and Peltier (1991), Peltier (1994) and Wu et al. (1998).

The zero line in the map of VCM nearly follows the Pacific coastal line; with a little curve in the north (Fig. 10). It is consistent in spatially long wavelengths with PGR models of ICE-3G (Tushingham and Peltier, 1991) and ICE-4G (Peltier, 1994), the rate of gravity changes (Pagiatakis and Salib, 2003), and the rate of geodetic height changes (CBN solution and Sella et al., 2007). The uplift rate in Yukon and Northern territories seen in the map of VCM (Fig. 10) is the artifact of the fitting, resulted from the poor distribution of data in those regions.

The Pacific coast of Canada is one of the few areas in the world where four tectonic plates meet and interact, and three different types of plate movements take place, resulting in significant earthquake activity. Plates move towards each other at converging, apart at diverging and past each other at transform boundaries. All three of these boundary types occur in offshore BC (Fig. 11).

About 200 km off the west coast of Vancouver Island, the Juan de Fuca plate and Pacific plate are diverging or spreading apart along the Juan de Fuca ridge. Further east, the Juan de Fuca plate is converging with and sliding (subducting) south of the North American plate at about 2–5 cm/year. This region, also called the Cascadia subduction zone, is located about 45 km south of Victoria, and about 70 km south of Vancouver (Fig. 12). Periodic giant mega thrust earthquakes exemplify a catastrophic sliding of the Juan de Fuca plate south of the North American plate (approximately once every 500 years). In the period between the mega-earthquakes, the Juan de Fuca plate continues trying (unsuccessfully) to slide south of the North American plate with the consequence that the rocks all along the edges of the plates are compressed or squeezed and uplifted, and these deformations are monitored using geodetic observations. Another small plate, the Explorer, is also sliding underneath the North American plate, and at the same time the Juan de Fuca plate is sliding along the Nootka fault. In the north, there is a major transform fault boundary between the Pacific and the North American plates called the Queen Charlotte fault. Therefore, the distinction between long-term tectonic trends and PGR in this region from the VCM map would be a nontrivial task.

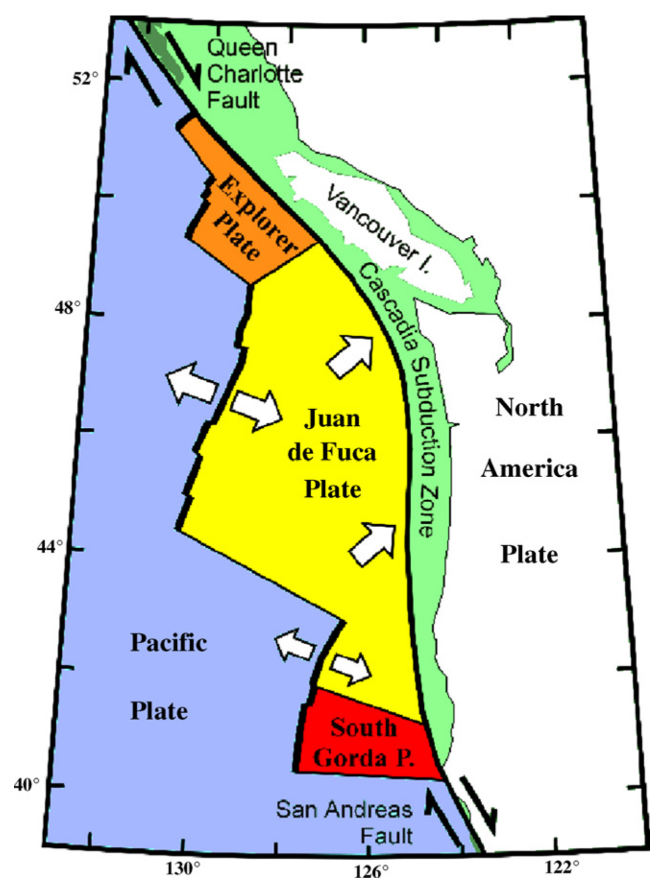

Fig. 11. The interaction of four tectonic plates in off shore BC.

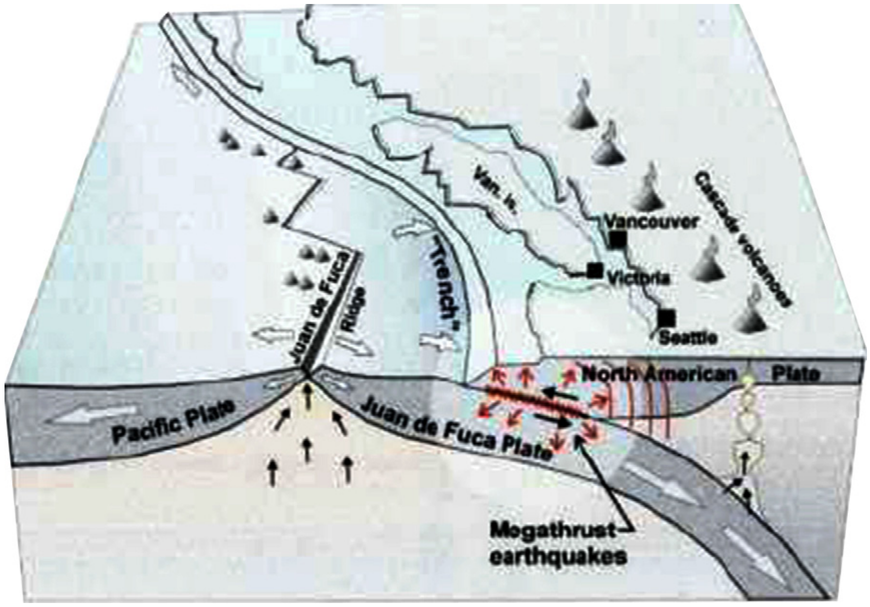

Fig. 12. Cascadia subduction zone: cross section (http://gsc.nrcan.gc.ca/geodyn/cascadia_e.php).

5. Conclusions and recommendation

A physically meaningful model of VCM was compiled for the whole of Canada in which the method of smooth piecewise algebraic approximation was applied. The VCM model is based on the simultaneous approximation of piecewise surfaces to scattered precise re-levelling data and tide gauge records.

In Eastern Canada, the PGR hinge line appears from Gulf of St. Lawrence in the map of VCM. It follows the Atlantic coast line to the south of the country and is in relatively good agreement with the map of rate of gravity changes (Pagiatakis and Salib, 2003) and rate of the geodetic height changes in CBN stations. In the Great Lakes, the relative movements or the tilt in this area varies between 0.5 and 1.5 mm/year per hundred kilometers along northeast–southeast direction, which is toward the maximum ice center in Hudson Bay. The computed tilt is in a relatively good agreement with the tilt obtained from GIA model of ICE-3G (Tushingham and Peltier, 1991) in this region (~1 mm/year per hundred kilometers). The zero line in our map is more to the North in the Great Lakes which might be due to the weight associated with the tide gauge records in the Churchill station. In fact, the trend of this tide gauge records gives the highest control to the absolute value of the VCM in the Great Lakes, and as such it is highly recommended that a more comprehensive study is carried on the records of Churchill tide gauge. The uplift in northern Great Lakes and subsidence in the south are compatible with the values of geodetic height changes from CBN and Sella et al. (2007) solutions.

The predicted rate of tilt in eastern prairies in Manitoba from VCM is in the range of 1.5–2 mm/year per hundred kilometers toward Hudson Bay. This solution is in good agreement with the results of previous studies for subsidence in southern Lake Athabaska in Saskatchewan and for uplift in southern prairies. The zero line in the map of VCM nearly follows the Pacific coastal line, which is consistent with the PGR zero line in the prairies. The oscillations of the uplift rate in Yukon, Yellowknife and all the way along the northern edge of the data are artifacts of the fitting in the edges of the area with poor distribution of data.

In general the map of VCM obtained from this study is in good agreement with the map of rate of gravity changes (Pagiatakis and Salib, 2003), and rate of geodetic height changes from GPS solutions (Sella et al., 2007).

Acknowledgements

We would like to thank Geodetic Survey Division (GSD), Natural Resource Canada for providing the Canadian first-order levelling data and Marine Environmental Data Service (MEDS) for providing us with monthly mean sea and lake level values. We acknowledge financial support provided by GEOIDE (GEOmatics for Informed DEcisions) Network of Centre of Excellence of Canada and CIDA (Canadian International Development Agency). Reviews by the anonymous reviewers greatly helped to improve the manuscript.

References

Adams, J., Basham, P.W., 1991. The seismicity and seismotectonics of Eastern Canada. In: Slemmons, D.B., Engdahl, E.R., Zoback, M.D., Blackwell, D.D. (Eds.), Neotectonics of North America, vol. 1. Geological Society of America, pp. 261–276.

Carrera, G., Vaníček, P., 1994. Compilation of a new map of recent vertical crustal movements in Canada. In: The 8th International Symposium on Recent Crustal Movements, Kobe, Japan, December 6–11, 1993.

Carrera, G., Vaníček, P., Craymer, M., 1991. The compilation of a map of recent vertical movements in Canada. Department of Surveying Engineering. Technical Report No. 153. University of New Brunswick, Fredericton, NB, Canada, p. 106.

Cartwright, D.E., 1983. On the smoothing of climatological time series, with application to sea-level at Newlyn. Geophys. J. Roy. Astronom. Soc. 75, 639–658.

Chrzanowski, A., Chen, Y.Q., Secord, J.M., 1986. Identification of deformation models in space and time domain. Surv. Rev. 33, 518–528.

Coordinating Committee on Great Lakes Basic Hydraulic and Hydrologic Data, 1977. Apparent Vertical Movements over the Great Lakes: Chicago. U.S. Army Corps of Engineers, and Cornwall, Ontario, Environmental Canada, 70 p.

Douglas, B.C., Kearney, M.S., Leatherman, S.P., 2001. Sea Level Rise; History and Consequences. Academic, San Diego.

Dyke, A.S., 2004. An outline of North American deglaciation with emphasis on central and northern Canada. In: Ehlers, J., Gibbard, P.L. (Eds.), Quaternary Glaciations—Extent and Chronology, Part 2, North America. Elsevier.

Godin, G., 1972. The Analysis of Tides. Liverpool Press, Liverpool.

Greiner, G., Hormann, K., 1996. Interpolating and approximating scattered 3D data with hierarchical tensor product splines. In A. Le Méhauté, C. Rabut, and L. L. Schumaker, Surface Fitting and Multiresolution Methods, 163–172.

Gregorski, B.F., Hamann, B., Joy, K.I., 2000. Reconstruction of B-spline surfaces from scattered data points. Proc. Computer Graphics International 2000, 163–170.

Henton, J., Craymer, M.R., Ferland, R., Dragert, H., Mazzotti, S., Forbes, D.L., 2006. Crustal motion and deformation monitoring of the Canadian landmass. Geomatica 60 (2), 173–191.

Holdahl, R.S., Hardy, R.L., 1978. Solvability and multiquadric analysis as applied to investigations of vertical crustal movements. Techtonophysics 52, 139–155.

Koohzare, A., 2007. A physical meaningful model of vertical crustal movements in Canada using smooth piecewise algebraic approximation: constraints for glacial isostatic adjustment models. Ph.D. Dissertation. University of New Brunswick.

Koohzare, A., Vaníček, P., Santos, M., 2006a. The use of smooth piecewise algebraic approximation in the determination of vertical crustal movements in Eastern Canada. In: Proceedings of the Joint Assembly of the IAG, IAPSO and IABO, vol. 130, Cairns, Australia.

Koohzare, A., Vaníček, P., Santos, M., 2006b. Compilation of a map of recent vertical crustal movements in Eastern Canada using geographic information system. J. Surv. Eng. ASCE 132 (4), 160–167.

Kumarapeli, P.S., 1985. Vestiges of Iapeton Rifting in the craton west of the northern Appalachian. Geosci. Can. 12 (2), 54–59.

Lambert, A., Courtier, N., Sasagawa, G.S., Klopping, F., Winester, D., James, T.S., Liard, J.O., 2001. New constraints on Laurentide postglacial rebound from absolute gravity measurements. Geophys. Res. Lett. 28, 2109–2112.

Lambert, A., James, T.S., Thorleifon, L.H., 1998. Combining geomorphological and geodetic data to determine postglacial rebound tilting in Manitoba. J. Paleolimol. 19, 365–376.

Lamontagne, M., Keating, P., Perreault, S., 2003. Seismotectonic characteristics of the lower St. Lawrence seismic zone, Quebec: insights from geology, magnetics, gravity, and seismics. Can. J. Earth Sci. 40, 317–336.

Lemieux, Y., Tremblay, A., Lavoie, D., 2003. Structural analysis of supracrustal faults in the Charlevoix area, Quebec: relation to impact cratering and the St-Laurent fault system. Can. J. Earth Sci./Rev. Can. Sci. Terre 40 (2), 221–235.

Liu, Q.W., Chen, Y.Q., 1998. Combining the geodetic models of vertical crustal deformation. J. Geod., 673–683.

Liu, Q.W., Parm, T., 1996. On the vertical deformation models. In: Proceedings of the 8th FIG International Symposium on Deformation Measurements, Hong Kong, June 25–28.

Mainville, A., Craymer, M., 2005. Present-day tilting of the Great Lakes region based on water level gauges. GSA Bull. 117 (7/8), 1070–1080.

Mazzoti, S., James, T.S., Henton, J., Adams, J., 2005. GPS crustal strain, postglacial rebound, and seismic hazard in eastern North America: The Saint Lawrence Valley example. J. Geophys. Res. 110 (b11), B11301.

Pagiatakis, S.D., Salib, P., 2003. Historical relative gravity observations and the time rate of change of gravity due to postglacial rebound and other tectonic movements in Canada. J. Geophys. Res. 108 (B9), 2406, doi:10.1029/2001JB001676.

Pan, M., Sjöberg, L.E., 1998. Unification of vertical datums by GPS and gravimetric geoid models with application to Fennoscandia. J. Geod., 64–70, doi:10.1007/s001900050149.

Park, K., Nerem, R.S., Davis, J.L., Schenewerk, M.S., Milne, G.A., Mitrovica, J.X., 2002. Investigation of glacial isostatic adjustment in the northeast U.S. using GPS measurements. Geophys. Res. Lett. 29 (11), 1509, doi:10.1029/2001GL013782.

Peltier, W.R., 1994. Ice age paleotopography. Science 265, 195–201.

Peltier, W.R., 1998. The inverse problem for mantle viscosity. Inverse Probl. 14, 441–478.

Peltier, W.R., 2002. On eustatic sea level history: last glacial maximum to holocene. Quater. Sci. Rev. 21 (1), 377–396 (20).

Randot, J., 1968. Nouvel impact meteoritique fossile, La structure semicirculaire de Charlevoia. J. Earth Sci. 5, 1305–1317.

Rapp, R., 1994. Separation between reference surfaces of selected vertical datums. J. Geod. 69, doi:10.1007/BF00807989.

Sella, G.F., Stein, S., Dixon, T.H., Craymer, M., James, T.S., Mazzotti, S., Dokka, R.K., 2007. Observation of glacial isostatic adjustment in "stable" North America with GPS. Geophys. Res. Lett. 34, doi:10.1029/2006GL027081.

Sella, G.F., Dixon, T.H., Mao, A., 2002. REVEL: a model for recent plate velocities from space geodesy. J. Geophys. Res. 107 (B4), 2081, doi:10.1029/2000JB000033.

Tackmam G., 1997. Postglacial tilting and lake level changes in Southern Manitoba. Ph.D. Thesis. University of Utah, Salt Lake City.

Tushingham, A.M., Peltier, W.R., 1991. Ice-3G: a new global model of late Pleistocene deglaciation based upon geophysical predications of postglacial relative sea level change. J. Geophys. Res. 96, 4497–4523.

Vaníček, P., 1976. Pattern of recent vertical crustal movements in Maritime Canada. Can. J. Earth Sci. 13, 661–667.

Vaníček, P., Christodulids, D., 1974. A method for evaluation of vertical crustal movements from scattered geodetic relevellings. Can. J. Earth Sci. 11, 605–610.

Vaníček, P., Carrera, G., 1993. Treatment of sea-level records in modeling linear vertical crustal motion. In: Proceedings of the CRCM'93, Kobe, Japan, pp. 305–309.

Vaníček, P., Nagy, D., 1981. On the compilation of the map of contemporary vertical crustal movements in Canada. Tectonophysics 71, 75–86.

Vaníček, P., Sjöberg, L.E., 1987. A note on vertical crustal movement determination techniques. Technical Report No. 9. Department of Geodesy, The Royal Institute of Technology, Stockholm.

Velicogna, I., Wahr, J., 2002. Postglacial rebound and Earth's viscosity structure from GRACE. J. Geophys. Res. 107, doi:10.1029/2001JB001735.

Wahr, J., DaZhong, H., Trupin, A., 1995. Predictions of vertical uplift caused by changing polar ice volumes on a viscoelastic earth. Geophys. Res. Lett. 22 (8), 977–980.

Wolf, D., 1985. An improved estimate of lithospheric thickness based on a reinterpretation of tilt data from Pleistocene Lake Algonquin. Can. J. Earth Sci. 22, 768–773.

Wu, P.P., Ni, Z., Kaufmann, G., 1998. Postglacial rebound with lateral heterogeneities: from 2-D to 3-D modeling. In: Wu, P. (Ed.), Dynamics of the Ice Age Earth: A Modern Perspective. Trans Tech Publications, Switzerland, pp. 557–582.

Zhou, J., Patrikalakis, N.M., Tuohy, S.T., Ye, X., 1997. Scattered data fitting with simplex splines in two and three dimensional spaces. The Visual Computer 13 (7), 295–315.